DOI: 10.17725/rensit.2021.13.479

Spin current and spin magnetoresistance of the heterostructure iridate/manganite interface

Gennady A. Ovsyannikov, Karen Y. Constantinian, Vladislav A. Shmakov, Yulii V. Kislinski, Andrey P. Orlov, Peter V. Lega

Kotelnikov Institute of Radioengineering and Electronics of RAS, http://www. cplire.ru/
Moscow 125009, Russian Federation

E-mail: gena@hitech.cplire.ru, karen@hitech.cplire.ru, shmakov-va@hitech.cplire.ru, yuli@hitech.cplire.ru, orl@cplire.ru, lega_peter@list.ru

Anton V. Shadrin

Moscow Institute of Physics and Technology, https://mipt.ru/
Dolgoprudny 141701, Moscow Region, Russian Federation
E-mail: shadrinant@mail.ru

Nikolay V. Andreev, Filipp O. Milovich

National Research Technological University "MISIS", https://misis.ru/
Moscow 119049, Russian Federation
E-mail: andreevn.misa@gmail.com, filippmilovich@mail.ru

Received Oktober 20, 2021, peer-reviewed Oktober 27, 2021, accepted November 08, 2021

Abstract: **The paper presents the results of fabrication and structural study of $SrIrO_3$/$La_{0.7}Sr_{0.3}MnO_3$ heterostructures. The results of experimental studies of the spin current arising in the regime of ferromagnetic resonance are presented. The spin-orbit interaction present in 5d-oxides of transition metals, which is $SrIrO_3$, provides an effective conversion of spin current to charge current due to the inverse spin Hall effect. The angular dependence of spin magnetoresistance makes it possible to determine the angle of the spin Hall effect.**

Keywords: **spin-orbit interaction, heterostructures, transition metals, topological symmetry, magnetoelectric effects**

PACS: 75.47.Lx, 75.25.-j

Acknowledgments: This work was carried out within the framework of the state task of the Kotel'nikov Institute of Radioengineering and Electronics of Russian Academy of Sciences and Russian Foundation for Basic Research No.19-07-00143. The study was carried out using the Unique Science Unit "Cryointegral" (USU #352529), which was supported by the Ministry of Science and Higher Education of Russia (Project No. 075-15-2021-667). Structural investigations were carried out using the equipment of the Center "Material Science and Metallurgy" with the financial support of Ministry of Education and Science of Russian Federation (№ 075-15-2921-696).

For citation: Gennady A. Ovsyannikov, Karen Y. Constantinian, Vladislav A. Shmakov, Anton V. Shadrin, Yulii V. Kislinski, Nikolay V. Andreev, Filipp O. Milovich, Angrey P. Orlov, Peter V. Lega. Spin current and spin magnetoresistance of the heterostructure iridate/manganite interface. *RENSIT: Radioelectronics. Nanosystems. Information technologies*, 2021, 13(4):479-486. DOI: 10.17725/rensit.2021.13.479.

Contents

1. INTRODUCTION

Significant progress in microelectronics in the field of informatics is due to the use of the charge properties of electrons. The use of electron spins opens up new opportunities in microelectronics, especially in the field of heat dissipation from submicron-sized elements. Spintronics elements enable solutions to the heat dissipation problem because there is no heat dissipation for spin transfer (spin current).

The detection and generation of spin current requires a completely different approach to the problem. A challenging task is the conversion of the spin current into a charge current, which is used in modern systems. The spin Hall effect is used to describe the conversion of spin current to charge current and vice versa in paramagnetic metals [1]. The conversion efficiency is determined by a parameter, the spin Hall effect angle θ_{SH}, which is defined as the ratio of the spin Hall resistance and the charge conduction of the paramagnetic metal. θ_{SH} can be determined from non-local magnetotransport measurements (see, for example [2]).

The most common method is to use spin pumping in a ferromagnetic resonance (FMR) mode in a paramagnetic metal/ferromagnet heterostructure [3-6]. However, a large number of parameters determining the magnitude of the spin current cannot be determined with good accuracy. As a result there is a strong scatter of experimentally obtained values of θ_{SH} for the same heterostructure. The number of parameters in the relationship between θ_{SH} and spin magnetoresistance is much smaller. As a result of spin resistance measurements it is possible to determine the value of θ_{SH} with greater accuracy.

The paper presents the results of fabrication and structural study of $SrIrO_3$/$La_{0.7}Sr_{0.3}MnO_3$ heterostructures, the results of experimental studies of the spin current arising in the regime of ferromagnetic resonance and magnetoresistance. The influence of anisotopic magnetoresistance and Rashba-Edelstein parameter on the parameters of heterostructures are discussed.

2. MANGANITE/IRIDATE HETEROSTRUCTURES

Thin films of strontium iridate $SrIrO_3$ and manganite $La_{0.7}Sr_{0.3}MnO_3$ of nanometer thickness were deposited on single-crystal substrates (110)$NdGaO_3$. Epitaxial films were grown by magnetron sputtering at substrate temperatures of 770-800°C in Ar and O_2 gas mixture at a total pressure of 0.3 mBar [5,6].

The crystal structure of the obtained heterostructures has been studied by *X*-ray diffraction analysis and transmission electron microscopy (TEM). A relatively thick platinum film was deposited on top of the heterostructure to avoid charge build-up. We will describe the crystal lattice of $SrIrO_3$ and $La_{0.7}Sr_{0.3}MnO_3$ as a distorted pseudo-cube with lattice parameters a_{SIO} = 0.396 nm and a_{LSMO} = 0.389 nm respectively [6].

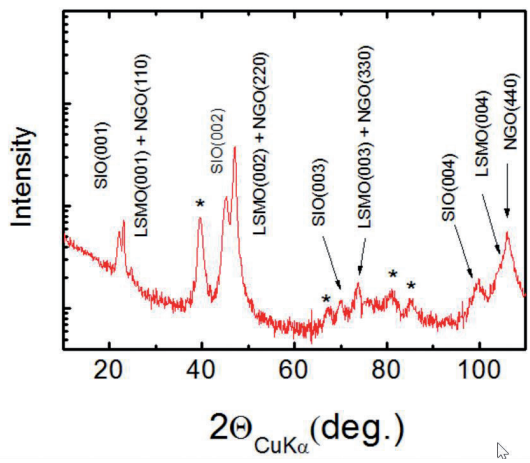

Fig. 1. *X-ray diffractogram of Pt/$SrIrO_3$/$La_{0.7}Sr_{0.3}MnO_3$/$NdGaO_3$. The reflections from the platinum film marked with an asterisk.*

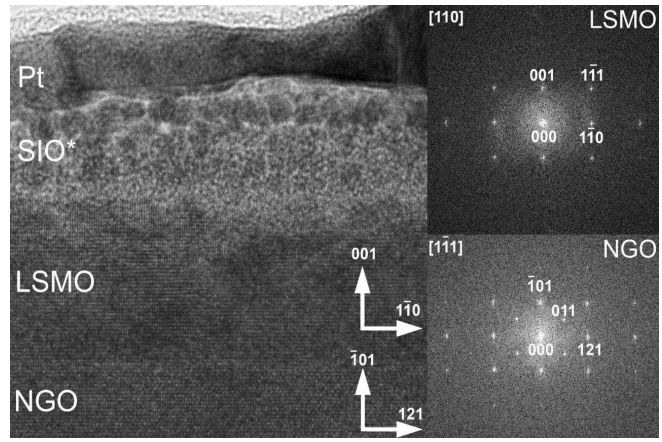

Fig. 2. *TEM image of a cross section of a $SrIrO_3$/$La_{0.7}Sr_{0.3}MnO_3$/$NdGaO_3$ (Pt/SIO/LSMO/NGO) heterostructure covered with a thick layer of platinum. The electron diffraction from the $NdGaO_3$ substrate regions and $La_{0.7}Sr_{0.3}MnO_3$ films are shown on the right.*

Fig. 1 shows a *X*-ray Bregg diffractogram of the obtained heterostructure. Multiple reflections from plane (001) of $SrIrO_3$ film, reflections (110) of $NdGaO_3$ substrate coinciding with reflections from plane (001) of $La_{0.7}Sr_{0.3}MnO_3$ as well as reflections from platinum film can be seen. Thus, it is possible to draw a conclusion that the growth of heterostructure is carried out by the "cube upon cube" mechanism with the following ratios: (001)$SrIrO_3$||(001) $La_{0.7}Sr_{0.3}MnO_3$||(110)$NdGaO_3$ and [100] $SrIrO_3$||[100]$La_{0.7}Sr_{0.3}MnO_3$||[001]$NdGaO_3$ [6].

Fig. 2 shows a TEM image of a cross section of a heterostructure obtained with a transmission electron microscope JEM −2100 at 200 kV. Elemental analysis was performed by *X*-ray energy dispersive system (OXFORD Instruments, INCA Energy). The cross section slice plate for transmission electron microscopy was made by using a focused ion beam in a Carl Zeiss CrossBeam Neon 40 EsB scanning electron-ion microscope equipped with an auto-emission electron and a gallium ion gun with a resolution of 1 and 7 nm. The unit was equipped with a micromanipulator and gas injection system for local precursor gas (Pt, W, etc.) deposition.

A layer of metal mask (Pt) up to 2 μm thick was formed on the sample surface to protect from damage. Ga^+ ions with an energy of 30 keV were used to obtain the slice and its thinning (polishing) with a gradual decrease of the etching current from 5 nA to 5 pA. To remove the amorphous layer at the final stage, the ion energy was decreased to 5 keV.

Presumably, during the preparation of the sample for TEM, the upper layer of $SrIrO_3$ was damaged - amorphized during the interaction with the beam of gallium ions. At the same time, the layer $La_{0.7}Sr_{0.3}MnO_3$ remained undamaged. In the high-resolution image, we can observe a clearly pronounced even boundary between the $La_{0.7}Sr_{0.3}MnO_3$ layer and the $NdGaO_3$ substrate. Hence, an epitaxial correspondence between the layer and the substrate is observed. The inset to the figure shows Fourier images from the

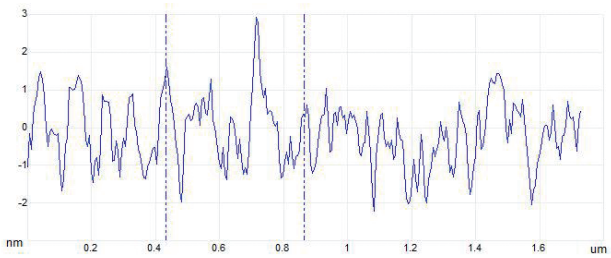

Fig. 3. *$La_{0.7}Sr_{0.3}MnO_3$ film surface taken on an atomic force microscope.*

regions of the figure corresponding to the substrate and $La_{0.7}Sr_{0.3}MnO_3$ layer, also confirming the epitaxial growth.

Fig. 3 shows a cross section of the $La_{0.7}Sr_{0.3}MnO_3$ film surface obtained using an atomic force microscope. Vertical irregularities 1-2 nm do not exceed the thickness of the upper $SrIrO_3$ film. Horizontally, the size of the irregularity is 50-70 nm.

3. SPIN CURRENT

The ferromagnetic resonance (FMR) line width characterizes the attenuation of the spin precession. In a ferromagnetic/normal metal heterostructure, an increase is observed due to the generation of a spin current across the interface [7]. Under microwave action in the FMR mode, a spin current j_S flows across the boundary in the ferromagnetic film, which is determined by the spin conductance of the boundary $g^{\uparrow\downarrow}$ and the amplitude of the magnetic moment precession m induced by the microwave magnetic field [4,8,9].

$$j_s = \frac{h}{8\pi}(mdm/dt)^2. \quad (1)$$

The value of the spin conductivity is usually determined from the increase in spin damping caused by the flow of a spin current. In our case the expression for the spin conductivity of the $SrIrO_3$/$La_{0.7}Sr_{0.3}MnO_3$ interface looks af following:

$$g^{\uparrow\downarrow} = \frac{4\pi\gamma_g M_s t_{LSMO}}{g\mu_B\omega_f}(\Delta H_{SIO/LSMO} - \Delta H_{LSMO}), \quad (2)$$

where $La_{0.7}Sr_{0.3}MnO_3$ film magnetization M_S = 300 Oe determined from resonance magnetic field value of FMR, t_{LSMO} = 12 nm film thickness $La_{0.7}Sr_{0.3}MnO_3$, μ_B = $9.274\cdot10^{-21}$ erg/G is the Bohr magneton, g = 2, γ_g = $17.605\cdot10^6$ $s^{-1}G^{-1}$ is the gyromagnetic ratio for free electrons and ω_f = $2\pi\cdot9.51\cdot10^9$ s^{-1} is the microwave frequency. At room temperature, the increase in the $\Delta H_{SIO/LSMO} - \Delta H_{LSMO}$ = 20 Oe width is 20 Oe, which gives $g^{\uparrow\downarrow}$ = $1\cdot10^{18}$ m^{-2} for $SrIrO_3/La_{0.7}Sr_{0.3}MnO_3$ heterostructures. Note that = $1.3\cdot10^{18}$ m^{-2} was obtained in [10] for $SrIrO_3$/$La_{0.7}Sr_{0.3}MnO_3$ heterostructure obtained by laser ablation.

Inverse spin Hall effect is used to detect spin current [3,8]. According to the effect the ratio of spin and charge currents is determined by a dimensionless parameter – the spin Hall angle θ_{SH}:

$$\vec{j}_{ISHE} = \theta_{SH}\frac{e}{\hbar}\left[\vec{n}\times\vec{j}_s^{\,0}\right], \quad (3)$$

where $\vec{n}$ is unit vector of spin momentum direction.

The voltage dependence on the upper film $V(H)$ is measured when the magnetic field is swept close to the resonance value of the FMR. **Fig. 4** shows the magnetic-field voltage dependence on the $SrIrO_3$ film under ferromagnetic resonance conditions at 2.6 GHz. The experimental dependence is well approximated by the following formula taking into account the effect of spin current and the contribution from anisotropic magnetoresistance (AMR) [11,12]:

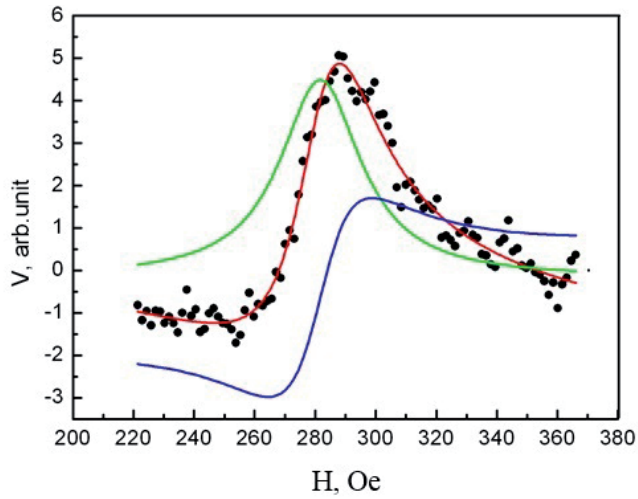

Fig. 4. *Spectrum of voltage induced by spin current, f = 2.6 GHz, T = 300 K. Red curve – approximation by Lorentz line and antisymmetrical component of anisotropic magnetoresistance, blue curve – antisymmetrical part of anisotropic magnetoresistance, green curve – sum of symmetrical part of anisotropic magnetoresistance and spin current signal.*

$$V = \left[V_{AMR}^{S} L(H) + V_{AMR}^{A} L'(H)\right] \sin 2\varphi_0 \sin \varphi_0 + \\ + V_Q L(H) \cos \varphi_0, \quad (4)$$

where $L(H) = \Delta H^2/[(H - H_0)^2 + \Delta H^2]$ is the symmetric Lorentz function, $L'(H) = \Delta H(H - H_0)/[(H - H_0)^2 + \Delta H^2]$ is the asymmetric Lorentz function, V_{AMR}^{S} and V_{AMR}^{A} are the amplitudes of both symmetric and asymmetric parts of the AMR contribution, $V_Q(H)$ is the voltage on the $SrIrO_3$ film, caused by spin current flowing through the interface, φ_0 is angle between external magnetic field and normal to voltage direction caused by reverse spin Hall effect. For $\varphi_0 = 45°$ assuming a ratio $V_{AMR}^{A}/V_{AMR}^{S} = -\mathrm{tg}\varphi_I \approx -1$ [11], where φ_I is the phase difference between microwave current and microwave magnetization from the amplitude V_{AMR}^{A} we obtain that the contribution from the spin current is less than 10% of the V_{AMR}^{S}.

4. SPIN MAGNETORESISTANCE

Magnetic-field dependence of the change in the normalised magnetoresistance (MR) of the heterostructure is shown in **Fig. 5***b*. The normalisation is given for resistance at $H = 0$. Directions of magnetic field change are indicated by arrows. The

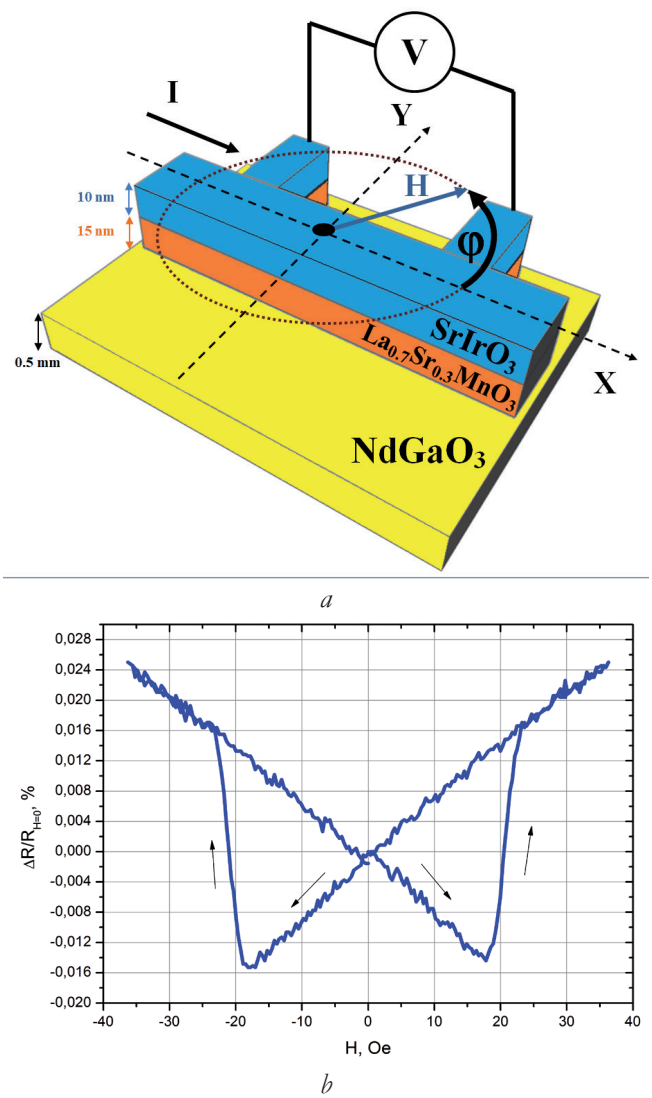

Fig. 5. *(a) The topology of the measurements $SrIrO_3/La_{0.7}Sr_{0.3}MnO_3$. (b) Magnetic-field dependence of variation of normalized magnetoresistance of heterostructures. The normalization is given for resistance at H = 0. The directions of magnetic field change are indicated by arrows.*

hysteresis of the magnetoresistance change can be seen. The maximum value of the MR variation is 0.032%. The field was directed perpendicular to the direction of the current flow (angle φ = 90° in the Fig. 5*a*).

The MR field dependence follows the manganite magnetisation curve [13]. The small value of the hysteresis loop width is probably caused by the proximity effect (penetration of the magnetic order parameter in the $La_{0.7}Sr_{0.3}MnO_3$ film into $SrIrO_3$).

Following the theory [14] taking into account conductivity of $La_{0.7}Sr_{0.3}MnO_3$ film the expression for spin resistance (SMR) is as follows [15]:

$$\frac{\Delta R}{R} = \frac{\theta_{SH}^2 \lambda_S g_R \tanh^2(t_{SIO}/2\lambda_S)}{(1+\eta)t_{SIO}[1+g_R \coth(t_{SIO}/\lambda_S)]}, \quad (5)$$

where θ_{SH} and λ_S are the spin angle and spin diffusion length in the $SrIrO_3$ film correspondingly. $\eta = \rho_{SIO}t_{LSMO}/\rho_{LSMO}t_{SIO} = 0.33$ are determined by the resistivities of iridate and manganite $\rho_{SIO} = 3\cdot10^{-4}$ Ωcm and $\rho_{LSMO} = 1.1\cdot10^{-3}$ Ωcm, and the thicknesses of these films $t_{LSMO} = 12$ nm and $t_{SIO} = 10$ nm, $g_R = h\rho_{SIO}\lambda_S g^{\uparrow\downarrow}/e^2$. Using the data for the spin resistance value of the boundaries [6] $g^{\uparrow\downarrow} = 10^{18}$ m^{-2} and the value $\lambda_S = 1$ nm we obtain $g_R = 0.12$. Under the condition $t_{SIO} >> \lambda_S$ relation (5) is simplified. Substituting the parameters calculated above we obtain $\theta_{SH} \approx 0.2$. Assuming that the anisotropic magnetoresistance (AMR) gives an additive contribution to the resistivity of the heterostructure together with the spin current we obtain that the value must be reduced to the root of the relationship between the amplitude of the symmetric AMR signal and the spin current signal in the ferromagnetic resonance $\sqrt{V_Q/V_{AMR}^S} = 0.3$ [6].

Along with the spin magnetoresistance there is the Rashba-Edelstein magnetoresistance which results from the processes occurring at the boundary with broken symmetry of the inversion [16-18]. Recently this effect has been investigated experimentally in a Bi/Ag/ ferromagnetic multilayer [19] caused by nonequilibrium spin accumulation at the interface

5. CONCLUSION

The structural parameters of the fabricated $SrIrO_3/La_{0.7}Sr_{0.3}MnO_3$ heterostructure were studied. Epitaxial growth of two films on $NdGaO_3$ substrate was observed by transmission electron microscope and confirmed by *X*-ray diffraction structure measurements. The value of the spin Hall angle was determined by two methods by direct measurement of the voltage induced by the spin current induced in the ferromagnetic resonance mode and by measuring the spin resistance. A strong influence of anisotropic magnetoresistance on the spin transport parameters was observed.

REFERENCES

1. Zhang S. Spin Hall Effect in the Presence of Spin Diffusion. *Phys. Rev. Lett.*, 2000, 85:393.
2. Mihajlovic G, Pearson JE, Garcia MA, Bader SD, and Hoffmann A. Negative Nonlocal Resistance in Mesoscopic Gold Hall Bars: Absence of the Giant Spin Hall Effect. *Phys. Rev. Lett.*, 2009, 103:166601.

3. Saitoh E, Ueda M, Miyajima H, and Tatara G. Conversion of spin current into charge current at room temperature: Inverse spin-Hall effect. *Appl. Phys. Lett.*, 2006, 88:182509.
4. Mosendz O, Vlaminck V, Pearson JE, Fradin FY, Bauer GEW, Bader SD, and Hoffmann A. Detection and quantification of inverse spin Hall effect from spin pumping in permalloy/normal metal bilayers. *Phys. Rev. B*, 2010, 82:214403.
5. Shaikhulov TA, Ovsyannikov GA, Demidov VV, Andreev NV. Magnetic and Resistive Properties of Magnetite/Iridate Heterostructures. *Journal of Experimental and Theoretical Physics,* 2019, 129:112.
6. Ovsyannikov GA, Shaikhulov TA, Stankevich KL, Khaydukov Yu, Andreev NV. Magnetism at an iridate/manganite interface: Influence of strong spin-orbit interaction. *Phys. Rev. B*, 2020, 102:144401.
7. Shaikhulov TA, Ovsyannikov GA. Attenuation of Spin Precession in Manganite/Normal Metal Heterostructures. *Physics of the Solid State*, 2018, 60:2231.
8. Tserkovnyak Ya, Brataas A, Bauer GEW. Enhanced Gilbert damping in thin ferromagnetic films. *Phys. Rev. Lett.*, 2002, 88:117601.
9. Fengyuan Yang and P. Chris Hammel. FMR-driven spin pumping in Y_3Fe5O_{12}-based structures. *J. Phys. D: Appl. Phys.*, 2018, 51:253001.
10. Crossley S, Swartz AG, Nishio K, Hikita Y, and Hwang HY. All-oxide ferromagnetic resonance and spin pumping with $SrIrO_3$. *Phys. Rev. B*, 2019, 100:115163.
11. Azevedo A, Vilela-Leao LH, Rodrıguez-Suarez RL, Lacerda Santos AF, Rezende SM. Spin pumping and anisotropic magnetoresistance voltages in magnetic bilayers: Theory and experiment. *Phys.Rev. B*, 2011, 83:144402.
12. Atsarkin VA, Borisenko IV, Demidov VV, Shaikhulov TA. Temperature dependence of pure spin current and spin-mixing conductance in the ferromagnetic—normal metal structure. *J. Phys. D*, 2018, 51:245002.
13. Ovsyannikov GA, Petrzhik AM, Borisenko IV, Klimov AA, Ignatov YA, Demidov VV, Nikitov SA. Magnetotransport characteristics of strained $La_{0.7}Sr_{0.3}MnO_3$ epitaxial manganite films. *Journal of Experimental and Theoretical Physics,* 2009, 108:48.
14. Chen Y-T, Takahashi S, Nakayama H, Althammer M, Goennenwein STB, Saitoh E, and Bauer GEW. Theory of spin Hall magnetoresistance. *Phys. Rev. B*, 2013, 87:144411.
15. Du Ye, Takahashi Saburo and Nitta Junsaku. Spin current related magnetoresistance in epitaxial Pt/Co bilayers in the presence of spin Hall effect and Rashba-Edelstein effect. *Phys. Rev. B*, 2021, 103:094419.
16. Manchon A, Koo HC, Nitta J, Frolov S M, and Duine RA. New perspectives for Rashba spin-orbit coupling. *Nat. Mater.,* 2015, 14:871.
17. Emori Satoru, T Nanianxiang, Belkessam Amine M, Wang Xinjun, Matyushov Alexei, Babroski D, Christopher J, Gao Yuan, Lin Hwaide, and Sun Nian X. Interfacial spin-orbit torque without bulk

spin-orbit coupling. *Phys. Rev. B*, 2016, 93:18040.

18. Akio Asami, Hongyu An, Akira Musha, Makoto Kuroda, and Kazuya Ando. Spin absorption at a ferromagnetic-metal/ platinum-oxide interface. *Physical Review B.*, 2019, 99:024432.
19. Kim J, Chen Y-T, Karube S, Takahashi S, Kondou K, Tatara G, and Otani Y. Evaluation of bulk-interface contributions to Edelstein magnetoresistance at metal/ oxide interfaces. *Phys. Rev. B*, 2017, 96:140409(R).